UNIVERSIDADE DE SÃO PAULO

INSTITUTO DE FÍSICA
CAIXA POSTAL 20516
01498 - SÃO PAULO - SP
BRASIL

PUBLICAÇÕES

IFUSP/P-481

RESOLUTION OF HYDRODYNAMICAL EQUATIONS FOR TRANSVERSE EXPANSIONS - II

by

Y. Hama and F.W. Pottag
Instituto de Física, Universidade de São Paulo

Agosto/1984

RESOLUTION OF HYDRODYNAMICAL EQUATIONS
FOR TRANSVERSE EXPANSIONS - II

Y. Hama and F.W. Pottag
Instituto de Física, Universidade de São Paulo,
São Paulo, Brasil

ABSTRACT

The three-dimensional expansion of an initially flat and hot disc is studied, by using the previously developped formalism. As expected, the results show that the "trivial" region is much more important in the case of transverse flows, unless the total energy M is much larger than the presently available values. As M increases, $\frac{dN}{d\xi}$ increases at the same time that its maximum moves outward giving an increasing $<\xi>$ which is close to the value estimated by Milekhin.

I. INTRODUCTION

The purpose of this note is to present some results which have been obtained by solving the hydrodynamical equations applied to studying the transverse flows of an initially flat and hot disc. Our version of hydrodynamics is the most orthodox one [1], except that the total energy of the system M need not to be equal to the incident energy, but rather it is an event-dependent fraction of the latter [2].

Many important questions should certainly be clarified if the results of such a study are to be applied with confidence to some realistic problem. Some of them would be a) What is the nature of the fluid? b) Is there local thermal equilibrium? c) Is hydrodynamics applicable to high-energy collisions, especially to hadron-hadron collisions? d) Which are the initial conditions? These questions are by themselves very complex, requiring each of them a thorough investigation, and we hardly expect to find satisfactory answers in a near future. So, for the time being, it is worthwhile asking a less fundamental although equally important question about what happens with a well defined fluid with equally well known initial conditions.

Why an orthodox version? First, because the model is simple and well defined enough that without additional hypotheses the initial conditions are determined and the hydrodynamical equations lead unambiguously to the solution. In some recent works [3] in which the initial conditions are modified by taking into account that the thermalization may occur at an instant $\tau_0 >> \Delta$, where Δ is essentially the Lorentz contracted thickness of the incident particles, it is assumed that $v = \frac{x}{t}$ for $\tau < \tau_0$ (which is an approximation valid for Khalatnikov's solution [4] for one-dimensional flows) and the energy density ε_0 at $\tau = \tau_0$ is guessed by using the experimental $\frac{dN}{dy}$. Evidently, this prescription gives the same final result as the orthodox one, although different in concept. This coincidence suggests, however, that in such models the temporal evolution of the fragments before their materialization could well be simulated by a fluid expansion for $\tau < \tau_0$, including here both the longitudinal and the transverse flows. Transverse movements of such fragments should always exist.

An additional argument for using an orthodox version is a good description it furnishes for several data. In a series of works [2,5-7], we have carried out comparisons of theoretical results obtained with its application to hadron-hadron collisions (where we always take the event-by-event fluctuation into account by considering the missing mass M instead of the total energy) and the corresponding experimental data. Other comparisons have been done by other authors*, giving nice agreements. These results encourage us to continuing the use of hydrodynamics to hadron-hadron collisions. However, it is clear that, if the present results are applicable to hadron-hadron collisions, then with some modifications they may also be useful to studying hadron-nucleus as well as nucleus-nucleus collisions.

The nature of the fluid is not clear, but according to the current view it could be a quark-gluon plasma (many people accept its formation only in nucleus-nucleus collisions). In such a case, a phase transition should occur, before arriving at the final products and, although we do not know any study of this kind, we believe that the effects such transition would cause to the fluid flow is of importance. Despite the uncertainty, we recall that, once hydrodynamics is accepted, both longitudinal and transverse expansions will always exist and results of a simple model like ours will always be useful to understand the general behaviour of the phenomenon.

*See for instance the review article [8].

In what follows, we will describe in the next Section the problem we have treated and a summary of the formalism which has been developped in a previous paper [9] and used here. In Sec. III, we will report some results we have obtained by the use of the above prescription. Conclusions will be drawn in Sec. IV.

II. SUMMARY OF THE FORMALISM

The object of our study is the transverse expansion of a flat disc of uniform thickness 2ℓ, radius $R >> \ell$, with a constant initial temperature $T_0 >> T_d$, where $T_d \cong m_\pi$ is the dissociation temperature. Due to the axial as well as the forward-backward symmetry of the system, the expansion will equally be symmetrical. The equations of relativistic hydrodynamics are

$$\partial_\mu T^{\mu\nu} = 0 \quad , \qquad (2.1)$$

where

$$\begin{cases} T^{\mu\nu} = (\varepsilon+p)u^\mu u^\nu - pg^{\mu\nu} \quad , \\ p = c_0^2\,\varepsilon \end{cases} \qquad (2.2)$$

and we take a constant sound velocity c_0 here.

As explained in Ref. [9], following Milekhin [10], we use the fact that the asymptotic one-dimensional solution of (2.1) is given by

$$\begin{cases} \alpha \cong \frac{1}{2} \ln \frac{t+x}{t-x} , \\ y = \ln \frac{T}{T_0} \cong -c_0^2 \ln \frac{\sqrt{t^2-x^2}}{\Delta} , \end{cases} \tag{2.3}$$

where $\Delta = \sqrt{\frac{1-c_0^2}{\pi}}\,\ell$, to introducing the coordinate system

$$\begin{cases} \tau = \sqrt{t^2-x^2} , \\ \alpha_0 = \mathrm{th}^{-1} \frac{x}{t} , \\ r = \sqrt{y^2+z^2} , \\ \phi = \tan^{-1} \frac{z}{y} . \end{cases} \tag{2.4}$$

If we further assume that

$$\alpha = \alpha_0 , \tag{2.5}$$

which is approximately verified as shown by eq. (2.3) (here we are implicity assuming that the transverse flows do not modify the longitudinal ones), then the transverse flows are separated from the longitudinal ones, resulting for the former the following equations which are to be solved within the boundaries indicated in Fig. 1 .

$$\begin{cases} \frac{\partial y}{\partial \tau} = -\frac{c_0^2 \mathrm{ch}^2\xi}{\tau} - \frac{c_0^2 \mathrm{sh}\xi\mathrm{ch}\xi}{r} + (1-c_0^2)\,\mathrm{sh}\xi\mathrm{ch}\xi \frac{\partial \xi}{\partial \tau} \\ \qquad + (\mathrm{sh}^2\xi - c_0^2\mathrm{ch}^2\xi)\frac{\partial \xi}{\partial r} , \\ \frac{\partial y}{\partial r} = \frac{c_0^2 \mathrm{sh}\xi\mathrm{ch}\xi}{\tau} + \frac{c_0^2 \mathrm{sh}^2\xi}{r} - (\mathrm{ch}^2\xi - c_0^2\mathrm{sh}^2\xi)\frac{\partial \xi}{\partial \tau} \\ \qquad - (1-c_0^2)\,\mathrm{sh}\xi\mathrm{ch}\xi \frac{\partial \xi}{\partial r} . \end{cases} \tag{2.6}$$

(Here, ξ is the transverse rapidity of the fluid).

The boundary conditions that the solution of our interest must satisfy are

a) $$\begin{cases} y = -\infty , \\ \xi = \infty , \end{cases} \tag{2.7a}$$

along the straight line $r = R + \tau$;

b) $$\begin{cases} y = -c_0^2 \ln \frac{\tau}{\Delta} , \\ \xi = 0 , \end{cases} \tag{2.7b}$$

along the straight line $r = R - c_0\tau$ for $\tau < \frac{R}{c_0}$; and

c) $$\xi = 0 \tag{2.7c}$$

along the symmetry axis $r = 0$ when $\tau > \frac{R}{c_0}$.

To solve the system (2.6), we first subtract the longitudinal part from y , by introducing a new variable $y_\perp$,

$$y = y_\perp - c_0^2 \ln \frac{\tau}{\Delta} . \tag{2.8}$$

Then, we rewrite (2.6) in the canonical form

$$\left\{\begin{aligned} &\frac{\partial\psi}{\partial\tau} + \frac{v_\perp + c_0}{1 + c_0 v_\perp}\frac{\partial\psi}{\partial r} + \frac{c_0^2\, v_\perp}{1 + c_0 v_\perp}\left[\frac{1}{r} - \frac{c_0}{\tau}\right] = 0 \\ &\frac{\partial\phi}{\partial\tau} + \frac{v_\perp - c_0}{1 - c_0 v_\perp}\frac{\partial\phi}{\partial r} + \frac{c_0^2\, v_\perp}{1 - c_0 v_\perp}\left[\frac{1}{r} + \frac{c_0}{\tau}\right] = 0 \quad , \end{aligned}\right. \tag{2.9}$$

where

$$\left\{\begin{aligned} \psi &= y_\perp + c_0\xi \quad , \\ \phi &= y_\perp - c_0\xi \quad , \end{aligned}\right. \tag{2.10}$$

and

$$v_\perp = \mathrm{th}\,\frac{\psi - \phi}{2c_0} \quad . \tag{2.11}$$

Now, we may integrate eqs. (2.9) along two families of characteristics which are given by

$$\left\{\begin{aligned} &\text{a)}\quad \frac{dr}{d\tau} = \frac{v_\perp + c_0}{1 + c_0 v_\perp} \quad , \\ &\text{b)}\quad \frac{dr}{d\tau} = \frac{v_\perp - c_0}{1 - c_0 v_\perp} \quad . \end{aligned}\right. \tag{2.12}$$

In applying this procedure, there appears a difficulty which is related with the fact that every characteristic (b) as given by (2.12) starts at the point $(\tau=0 \, , \, r=R)$, where both ψ and ϕ are undefined. One possibility to overcome this difficulty is to round the sharp edge at $r=R$ as has been done by Baym et al. in a recent work [11], so that every point of the axis $\tau=0$ (or of a straight line $\tau = \tau_0$ in their case) becomes the initial point of a particular characteristic line (b). All the fluid begins to expand radially at that instant.

We have instead solved the problem, by using the ultrarelativistic solution

$$\left\{\begin{aligned} \psi &\cong \frac{c_0^2}{1+c_0}\,\ell n\left[\frac{R - c_0(\tau - r)}{(1 + c_0)r}\left(\frac{(1+c_0)\tau}{R+\tau-r}\right)^{c_0}\right] \quad , \\ \phi &\cong \frac{c_0^2}{1-c_0}\,\ell n\left[\frac{R - c_0(\tau - r)}{(1 + c_0)r}\left(\frac{R+\tau-r}{(1+c_0)\tau}\right)^{c_0}\right] \end{aligned}\right. \tag{2.13}$$

in the neighbourhood of $(\tau=0 \, , \, r=R)$ as the initial values.

Once the hydrodynamic equations are solved, we can now compute the transverse rapidity distribution of the fluid and the inclusive particle distributions. These quantities are calculated on the hypersurface $T = T_d$, where the final particles emerge free of interaction. We have

$$dN = n u^\mu d\sigma_\mu \Big|_{T=T_d} \quad , \tag{2.14}$$

where, in our approximation,

$$u^\mu = (\mathrm{ch}\xi \, , \, 0 \, , \, \mathrm{sh}\xi \, , \, 0) \tag{2.15}$$

and the components of the surface element $d\sigma_\mu$ are given by

$$d\sigma_\mu = \tau r d\alpha_0 d\phi(-dr \, , \, 0 \, , \, d\tau \, , \, 0) \tag{2.16}$$

(here, we included in $d\sigma_\mu$ the factor $\sqrt{-g} = \tau r$ which arises because of the curvilinear coordinates).

By replacing u^μ and $d\sigma_\mu$ in eq. (2.14) by (2.15) and (2.16) respectively and using the azimuthal symmetry and our assumption (2.5), we arrive at

$$dN = -2\pi n \frac{\tau r}{\left|\frac{\partial(\xi,y)}{\partial(\tau,r)}\right|} \left\{ sh\xi \frac{\partial y}{\partial r} + ch\xi \frac{\partial y}{\partial \tau} \right\}\Bigg|_{T=T_d} d\xi\, d\alpha \,. \qquad (2.17)$$

As for the inclusive particle distributions (with fixed M), Cooper and Frye's prescription [12] gives

$$E\frac{dN}{d\vec{p}} = \frac{g}{(2\pi)^3} \int \frac{p^\mu d\sigma_\mu}{\exp(\bar{E}/T_d) \pm 1}$$

$$= \frac{gm}{(2\pi)^3} \iiint_{T=T_d} \frac{\tau r \left[shy_\perp d\tau - ch(y_\parallel-\alpha)\, chy_\perp dr \right] d\alpha d\phi}{\exp\left\{\frac{m}{T_d}\left[ch(y_\parallel-\alpha)\, chy_\perp ch\xi - shy_\perp sh\xi\cos\phi\right]\right\} \pm 1} \,, \qquad (2.18)$$

where g is the statistical factor.

III. SOME NUMERICAL RESULTS

In this Section, we report some preliminary results which have been obtained with the application of the preceding formalism to hadron-hadron collisions. Then, the parameters R and ℓ have been fixed equal to

$$\begin{cases} R = \dfrac{1}{m_\pi} \,, \\ \ell = \dfrac{M}{m_p} R \,. \end{cases} \qquad (3.1)$$

We have also taken $c_0 = \frac{1}{\sqrt{3}}$ throughout the present calculation.

In order to study the energy dependence of the transverse flows, we have considered in this paper two arbitrary values of M ($M = 300$ GeV and $M = 1000$ GeV), for which we have obtained the transverse-rapidity distribution $\frac{dN}{d\xi}$ and the

mean rapidity $\langle\xi\rangle$.

Since eqs. (2.9) as well as the boundary conditions for ψ and ϕ are independent of M, the solution of this boundary value problem depends only on the radius R. The M dependence of the experimentally observed quantities, such as $\frac{dN}{d\xi}$, $\langle\xi\rangle$, $E\frac{dN}{d\vec{p}}$, ... appears only when the longitudinal part of y as given by eq. (2.8) is taken into account.

We show in Figs. 2 and 3 the radial distribution of $T_\perp \equiv e^{y_\perp}$ and ξ, respectively, at different instants of time. As can be perceived in Fig. 2, the contour of the fluid expands quickly and, at the same time, first the one-dimensional -flow region decreases until its disappearance at $\tau = \frac{R}{c_0}$ and then the transverse "temperature" $T_\perp$ decreases in the central region, developping a depression there, just like in the purely one-dimensional-flow case. However, as expected the "trivial" region is much more important in the present case as compared with the one-dimensional-flow case. In Fig. 3, one sees a rapid expansion of large-ξ components, which is consistent with the behaviour of $T_\perp$ as seen in Fig. 2; an initially fast slowing-down at $r \geq R$ followed by a gradual acceleration; and at the central region a less slow acceleration, which however changes the sign at larger τ.

The same results above are shown in Figs. 4 and 5, but this time as functions of τ at different spatial points. As can be seen in Fig. 4, $T_\perp(0)$ diminishes quickly after the interval $\frac{R}{c_0}$ during which it remains constant. In Fig. 5, the behaviour which has been described in connection with Fig. 3 appear more clearly, especially the rapid decrease of ξ at $r \gtrsim R$ followed by its gradual increase, an inflection at a certain value of τ and a slowing down. In Fig. 3, this latter characteristic appeared only in the small-r region, but now we can see that this is the general feature. If one compares Fig. 5 with Fig. 1 and Fig. 10, one notices that the change in the sign of $\frac{d\xi}{d\tau}$ mentioned above occurs just along A of Fig. 1, where the flow becomes non-trivial.

Until this point, we have shown only the transverse "temperature" $T_\perp$, but in order to compute the rapidity distribution, it is necessary to consider also the longitudinal part, which is, according to (2.3) and (2.8),

$$T_{\shortparallel} \equiv T_0 \, e^{-c_0^2 \, \ell n \frac{\tau}{\Delta}} = T_0 \left(\frac{\Delta}{\tau}\right)^{c_0^2} . \qquad (3.2)$$

The distribution of $T = T_{\shortparallel} T_\perp$ depends on the mass M of the system as shown by Figs. 6 and 7 for the two values we have considered here. The ξ-distribution remains evidently independent of M. One sees in these figures that, as expected, the cooling due to the longitudinal expansion is much more important and it increases with M. These figures are similar to those presented in Ref. [11], although the objects are quite different in size and the initial conditions seem to be unlike. One can even see an approximate scaling in the variables $\frac{r}{R}$ and $\frac{\tau}{R}$, if the correct initial temperature T_0 is taken in each case. The scaling would be exact if the initial conditions were the same in these variables, neglecting evidently small discrepancies due to numerical approximations.

The computation of $\frac{dN}{d\xi}$ (as well as $E\frac{dN}{d\vec{p}}$ - which will not be reported in this note), is performed over the hypersurface $T = T_d$. In Figs. 8 and 9, we show some of the isotherms for the values of M we are considering. The curves indicated with y_d are those which correspond to the dissociation

temperature, which we have taken $T_d = m_\pi$ in this paper. One sees again in these figures the importance of the "trivial"-flow region.

In Fig. 10, we show some of the curves with constant transverse rapidity ξ in the τr plane. The transverse rapidity distribution $\frac{dN}{d\xi}$ is then computed with the use of eq. (2.17) and Figs. 8 (or 9) and 10. The results so obtained are finally given in Fig. 11. One must recall that, due to our approximation expressed by eq. (2.5), the particle distribution as given by eq. (2.17) is independent of α, which is not exact. So, in the last step of computation of $\frac{dN}{d\xi}$, one may either consider an approximate α-dependence through the one-dimensional solution or just ignore the α-dependence and renormalize $\frac{dN}{d\xi}$ using the average multiplicity. Here, we have chosen the second alternative.

Figure 11 shows that, as M increases, $\frac{dN}{d\xi}$ increases in height and at the same time the position of the maximum moves outward, just as expected on the intuitive ground. We have calculated the average values of ξ and $<\xi>$, which are compared with Milekhin's results [10], in Table I.

IV. CONCLUSIONS

In the present work, we have studied the transverse expansion of an initially hot and flat disc, by using the previously developped formalism [9].

As shown in the preceding section, although it is by no means negligible, the transverse expansion is a small correction to the longitudinal one, especially at the central region (r - 0), being thus justified our procedure. In opposition to the longitudinal-flow case, the "trivial" region is much more important now, at least up to $M \cong 1$ TeV, which is one of the values we have considered here. As expected, $\frac{dN}{d\xi}$ (and indeed also $E\frac{dN}{d\vec{p}}$) becomes flatter when M increases, which is in accordance with Milekhin's estimate [10] and also with $\bar{p}p$-collider's data [13]. However, in comparison with the estimate in [10], a slightly faster increase of $sh\langle\xi\rangle$ is observed in our work.

Details of numerical computation will be reported by one of us [F.W.P.] in his doctor thesis and further results such as $E\frac{dN}{d\vec{p}}$ will be given both there and in a separate publication.

REFERENCES

[1] L.D. Landau, Izv. Akad. Nauk SSSR Ser. Fiz. 17 (1953) 51; Collected papers, ed. D. Ter Haar (Pergamon, Oxford, 1965) p. 569.

[2] Y. Hama, Phys. Rev. D19 (1979) 2623.

[3] K. Kajantie and L. McLerran, Phys. Lett. 119B (1982) 203; J.D. Bjorken, Phys. Rev. D27 (1983) 140.

[4] I.M. Khalatnikov, Zhur. Eksp. Teor. Fiz. 27 (1954) 529.

[5] Y. Hama and F.W. Pottag, Rev. Bras. Fís. 12 (1982) 247.

[6] Y. Hama and F.S. Navarra, Phys. Lett. 129B (1983) 251.

[7] Y. Hama and F.S. Navarra, Correlation between Charged-Particle Multiplicities and Pseudo-Rapidity Distributions in Hydrodynamical Cluster Model, to be published on Zeit. Phys. C.

[8] E.V. Shuryak, Phys. Rep. 61 (1980) 71.

[9] Y. Hama and F.W. Pottag, Resolution of Hydrodynamical Equations for Transverse Expansions - I, preprint IFUSP/P-479, Univ. de São Paulo (Brazil).

[10] G.A. Milekhin, Sov. Phys. JETP 35 (1959) 829.

[11] G. Baym et al., Nucl. Phys. A407 (1983) 541.

[12] F. Cooper and G. Frye, Phys. Rev. D10 (1974) 186.

[13] UA1 Collaboration, G. Arnison et al., Phys. Lett. 118B (1982) 167.

FIGURE CAPTIONS

Fig. 1 - Proper-time evolution of the two families of characteristics given by eqs. (2.12). Regions of different flow-regime are indicated with (I) one-dimensional-flow region; (II) "trivial" three-dimensional-flow region; and (III) non-trivial three-dimensional-flow region.

Fig. 2 - Radial distribution of $T_\perp \equiv e^{y_\perp}$ at different instants of time indicated. The spike close to the end of each curve is due to the numerical approximation used and has no physical meaning. Both r and τ are expressed in units of GeV^{-1} ($\hbar = c = k = 1$).

Fig. 3 - Radial distribution of the transverse rapidity ξ at different instants. r and τ are expressed in units of GeV^{-1}.

Fig. 4 - Time evolution of $T_\perp \equiv e^{y_\perp}$ at different points. The spike close to the beginning of each curve ($r > R$) is due to the numerical approximation used and has no physical meaning. r and τ are expressed in units of GeV^{-1}.

Fig. 5 - Time evolution of ξ at different points. r and τ are expressed in units of GeV^{-1}.

Fig. 6 - Radial distribution of T/T_0 at different instants indicated for $M = 300$ GeV. r and τ are given in units of GeV^{-1}.

Fig. 7 - Radial distribution of T/T_0 at different instants indicated for $M = 1000$ GeV. r and τ are given in units of GeV^{-1}.

Fig. 8 - Some isotherms are shown in the τr-plane for $M = 300$ GeV. The broken line indicates the one with $T = T_d = m_\pi$. τ and r are given in units of GeV^{-1}.

Fig. 9 - Some isotherms are shown in the τr-plane for $M = 1000$ GeV. The broken line indicates the one with $T = T_d = m_\pi$. τ and r are given in units of GeV^{-1}.

Fig. 10 - Curves with constant ξ are shown in the τr-plane.

Fig. 11 - Transverse-rapidity distribution at 2 values of M as indicated.

TABLE I

M (GeV)	$\langle\xi\rangle$	$sh\langle\xi\rangle$	$sh\langle\xi\rangle_{Milekhin}$
300	0.928	1.067	1.150
1000	1.143	1.409	1.365

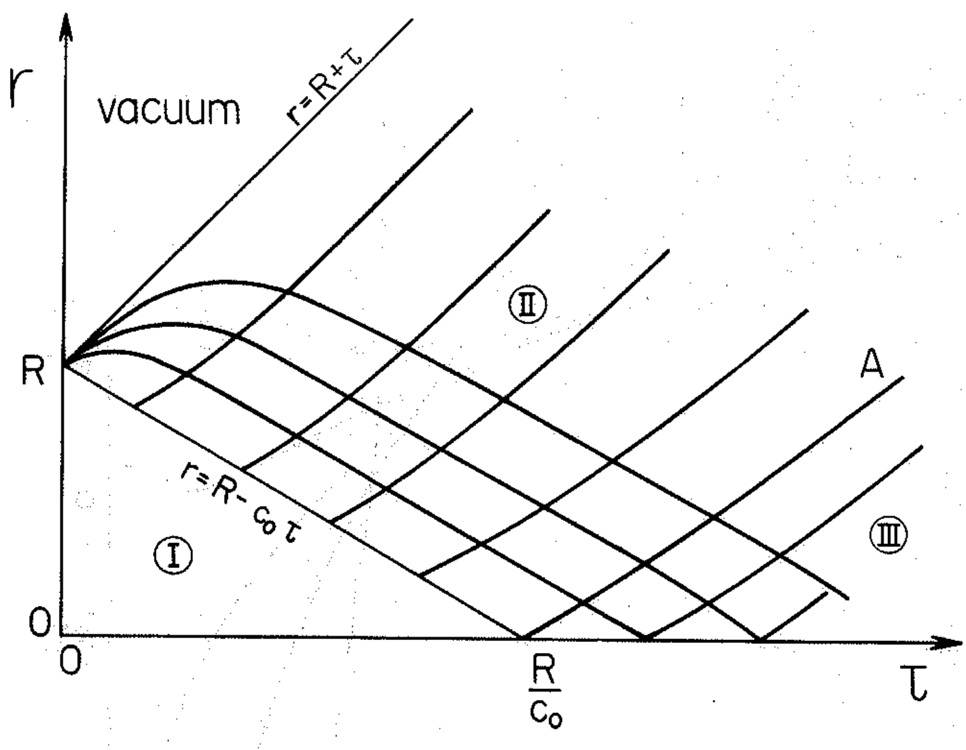

FIG. 1

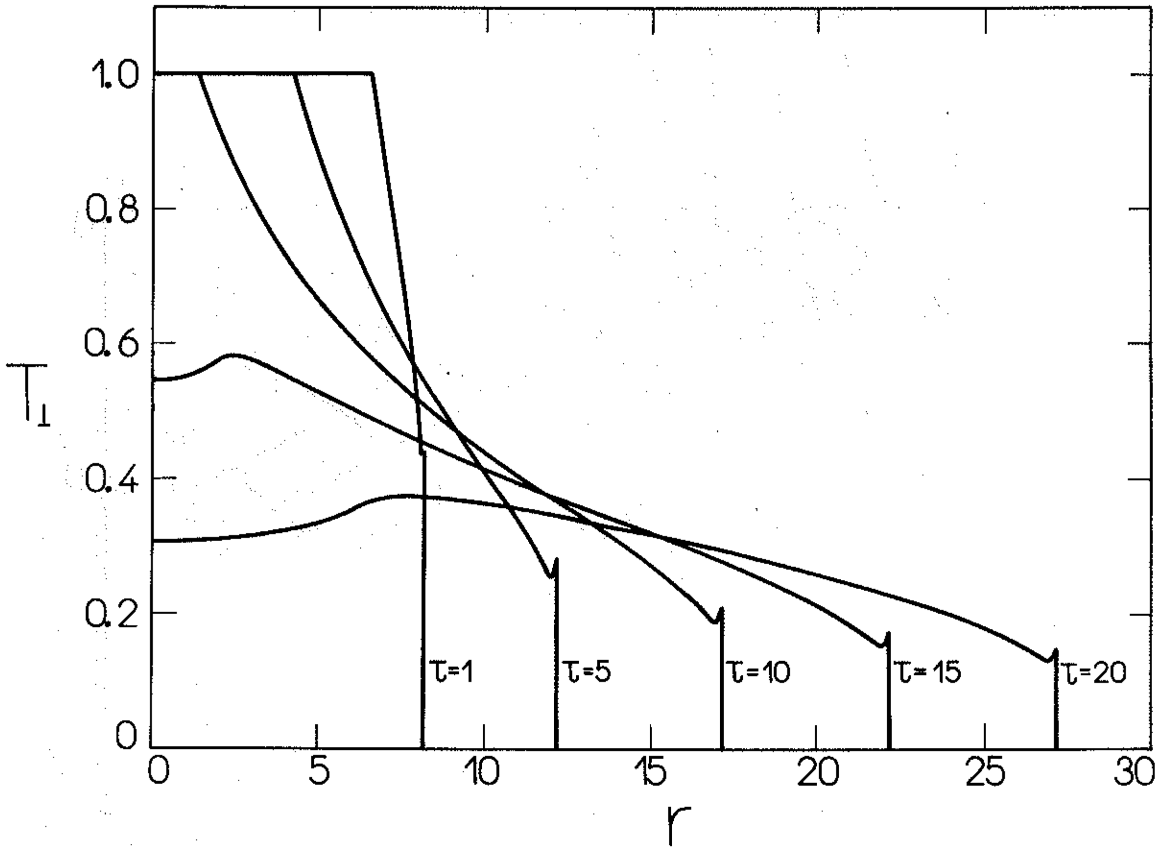
1.0
0.8
0.6
0.4
0.2
0
$T_\perp$
$\tau=1$
$\tau=5$
$\tau=10$
$\tau=15$
$\tau=20$
0
5
10
15
20
25
30
r

FIG. 2

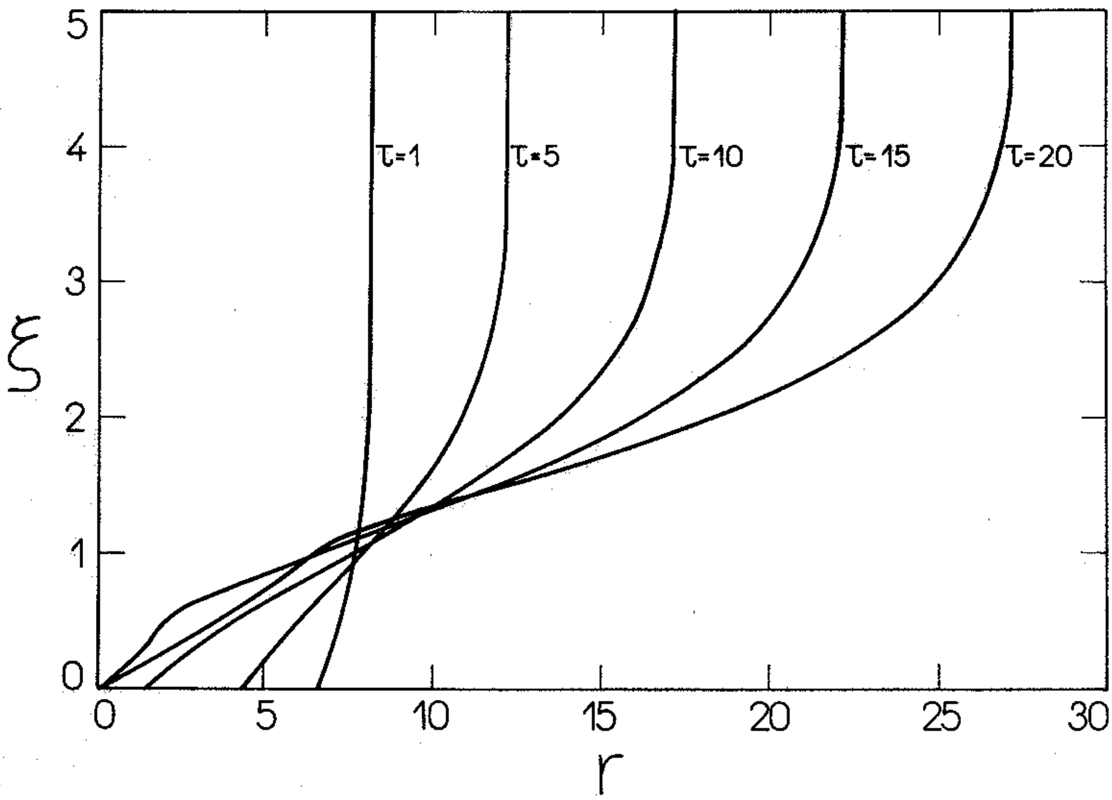
5
4
3
2
1
0
ξ
$\tau=1$
$\tau=5$
$\tau=10$
$\tau=15$
$\tau=20$
0
5
10
15
20
25
30
r

FIG. 3

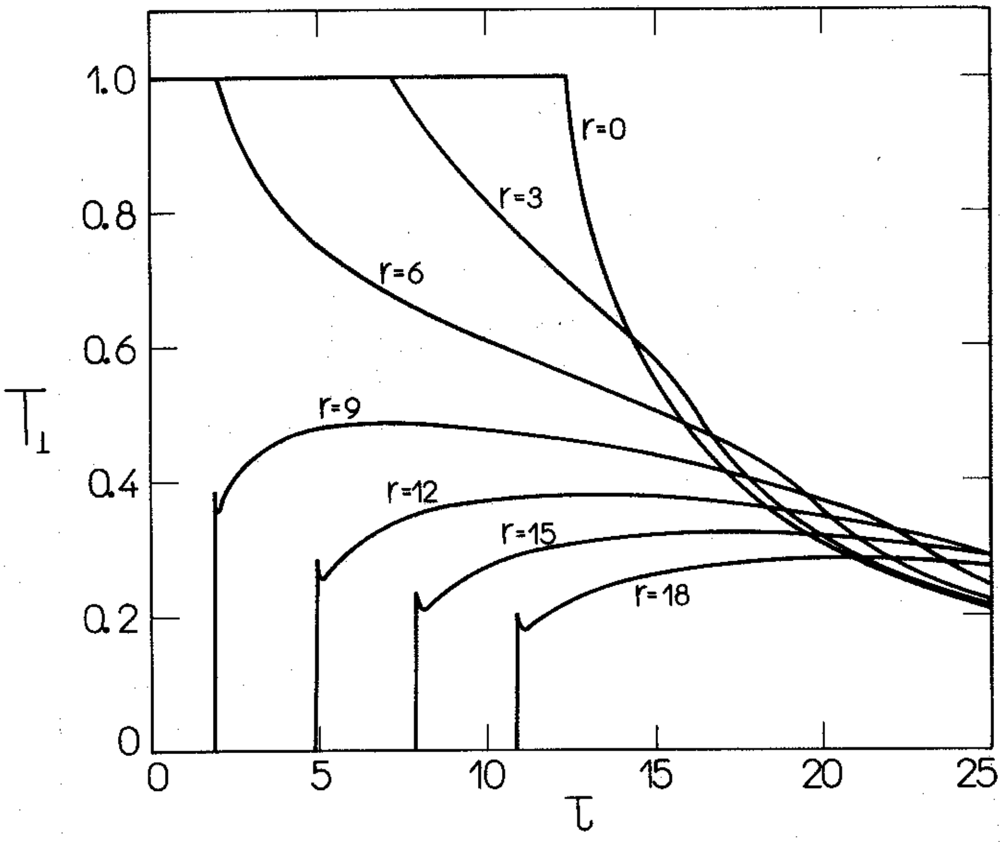

1.0
0.8
0.6
0.4
0.2
0
0
5
10
15
20
25
$T_\perp$
τ
r=0
r=3
r=6
r=9
r=12
r=15
r=18

FIG. 4

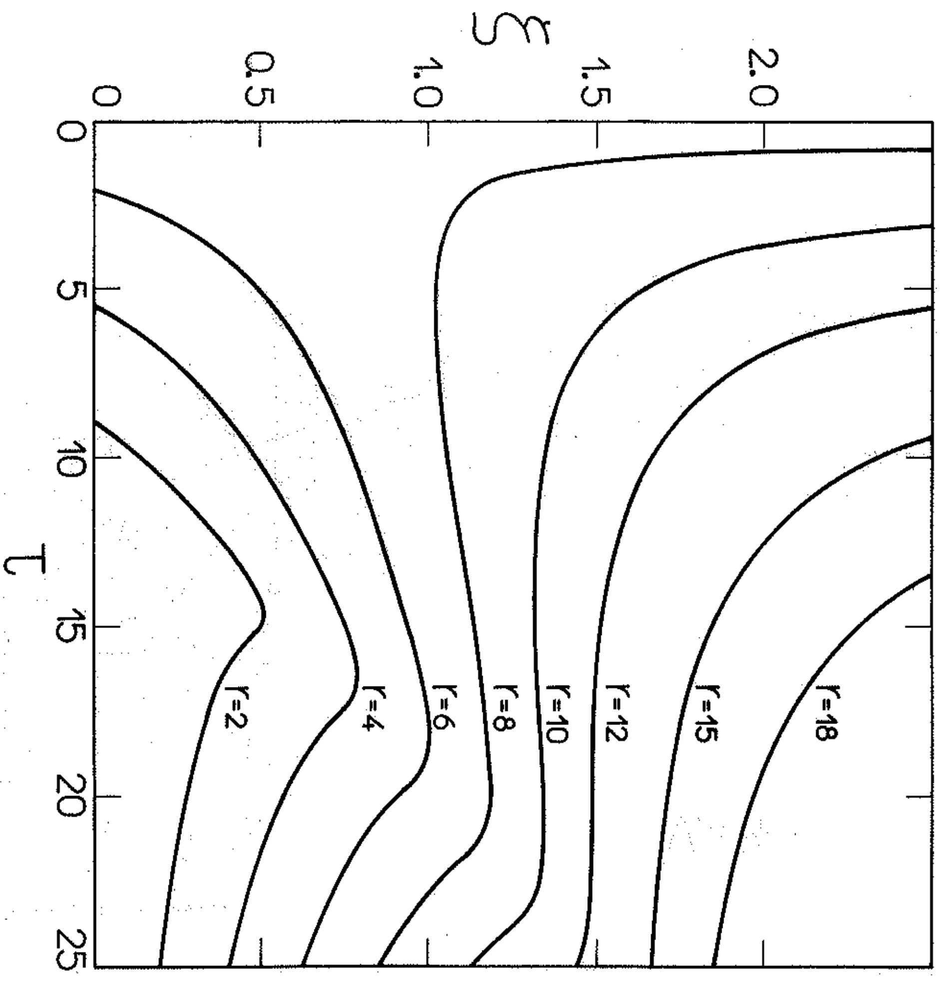

ξ
0
0.5
1.0
1.5
2.0
0
5
10
15
20
25
τ
r=2
r=4
r=6
r=8
r=10
r=12
r=15
r=18

FIG. 5

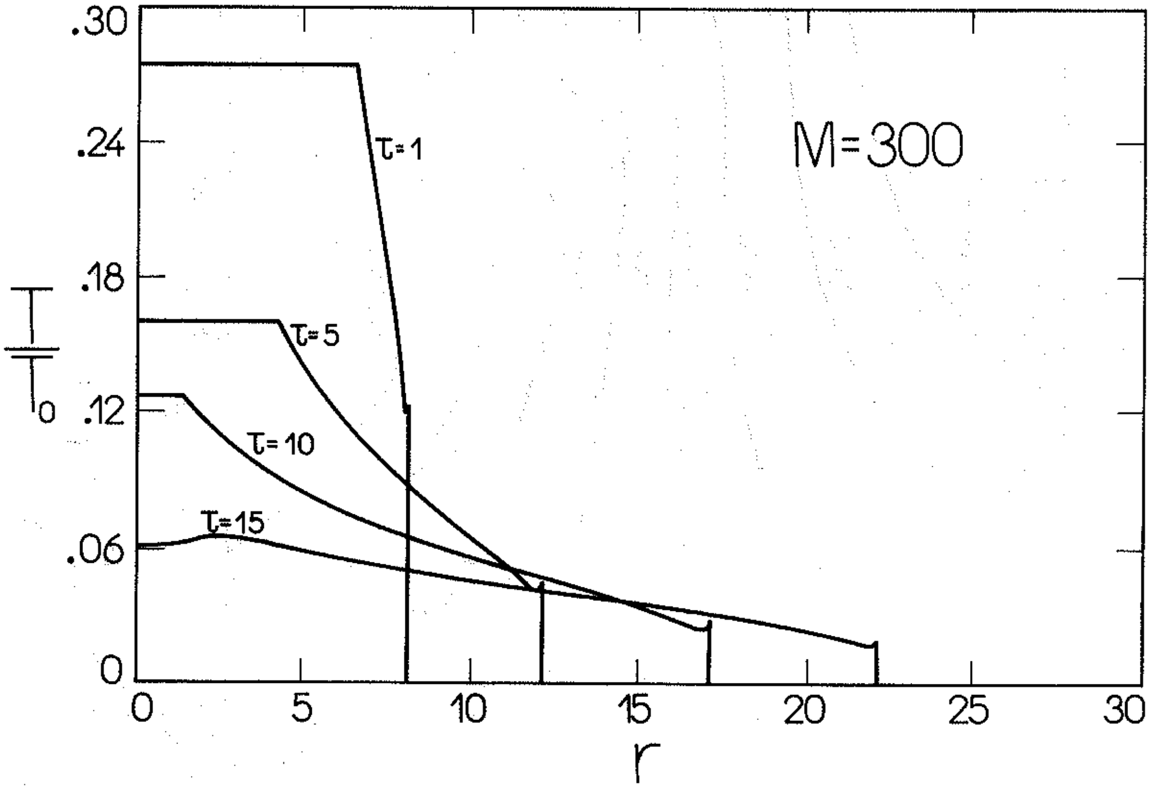
M=300
τ=1
τ=5
τ=10
τ=15
T/T0
r
.30
.24
.18
.12
.06
0
0
5
10
15
20
25
30
FIG. 6

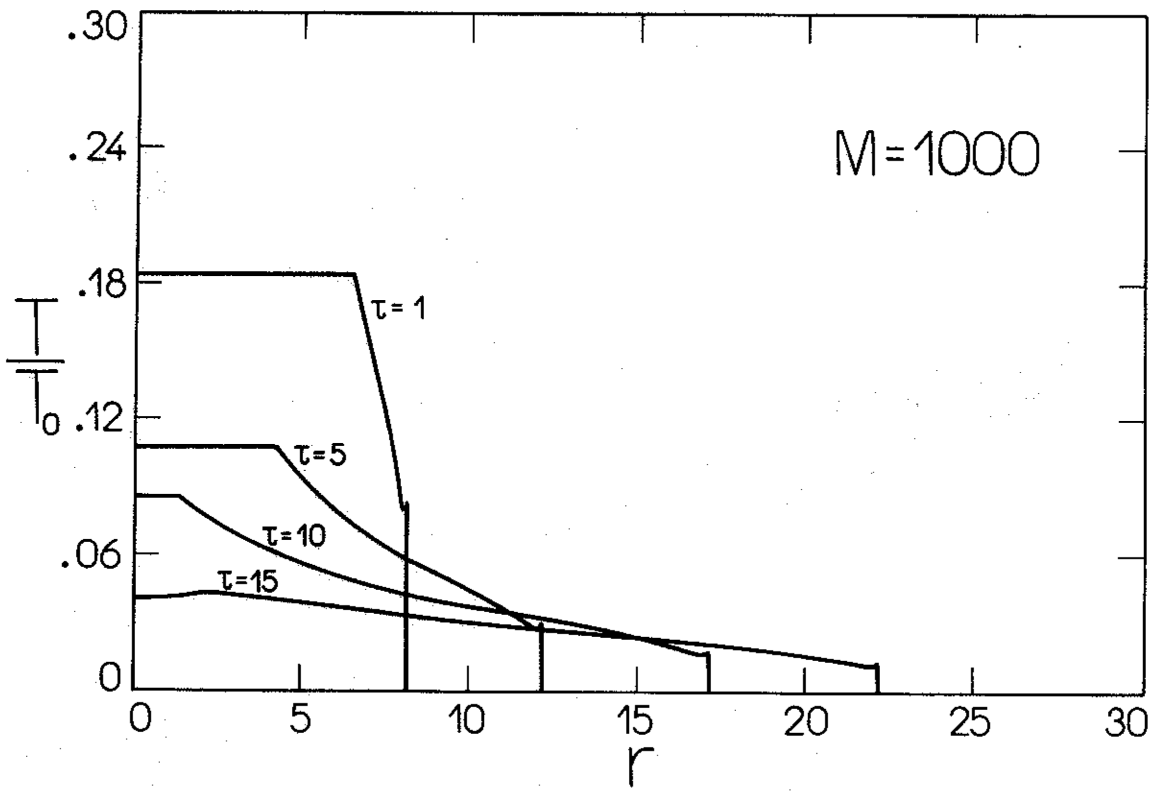
M=1000
τ=1
τ=5
τ=10
τ=15
T/T0
r
.30
.24
.18
.12
.06
0
0
5
10
15
20
25
30
FIG. 7

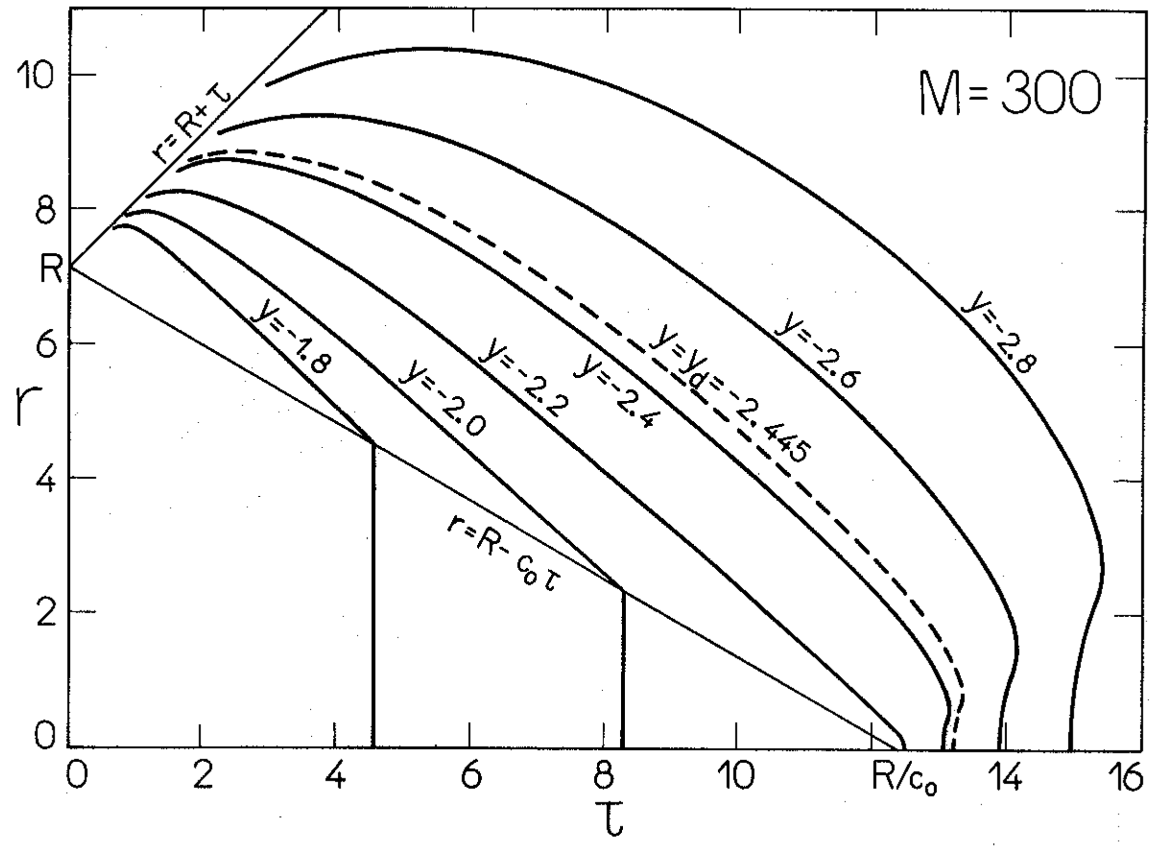
M= 300
r=R+τ
y=-1.8
y=-2.0
y=-2.2
y=-2.4
y=y_d=-2.445
y=-2.6
y=-2.8
r=R-c_0τ
R
r
τ
R/c_0
0
2
4
6
8
10
14
16

FIG. 8

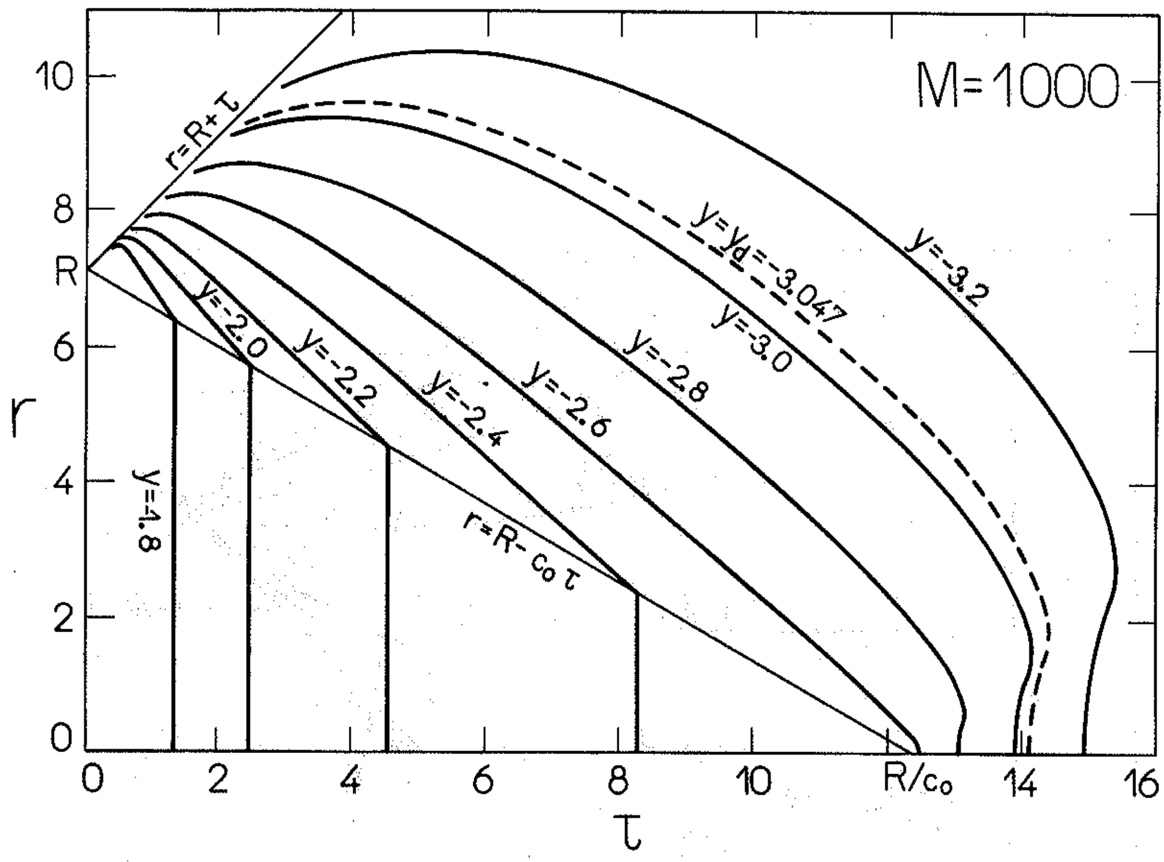
M=1000
r=R+τ
y=-1.8
y=-2.0
y=-2.2
y=-2.4
y=-2.6
y=-2.8
y=-3.0
y=y_d=-3.047
y=-3.2
r=R-c_0τ
R
r
τ
R/c_0
0
2
4
6
8
10
14
16

FIG. 9

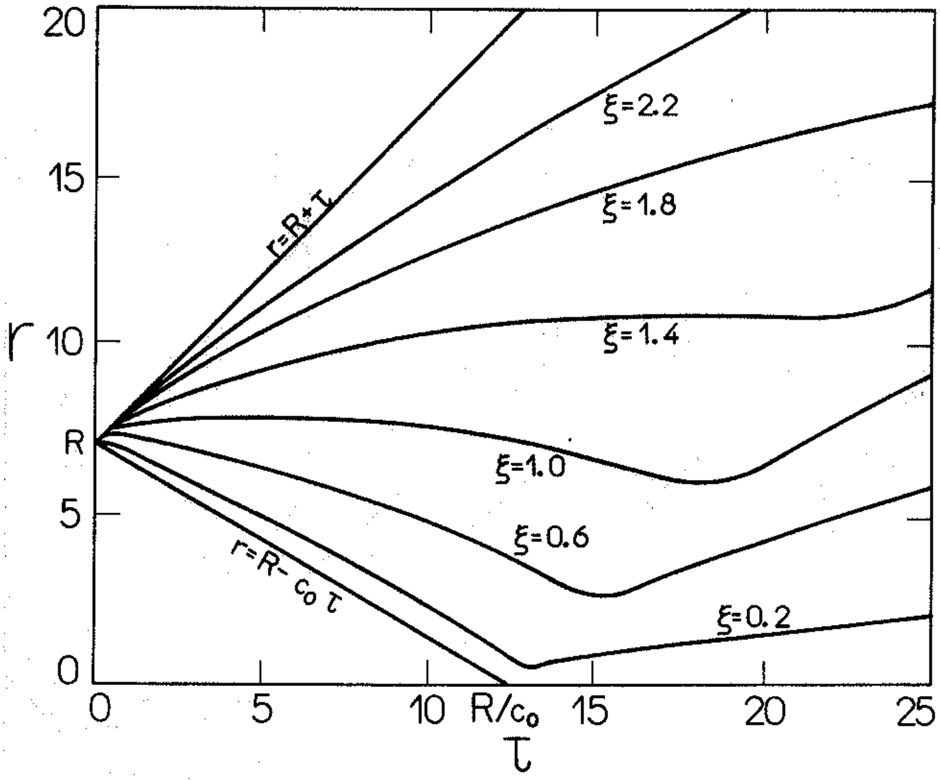

r
τ
20
15
10
R
5
0
0
5
10
R/c_0
15
20
25
r=R+τ
r=R− c_0 τ
ξ=2.2
ξ=1.8
ξ=1.4
ξ=1.0
ξ=0.6
ξ=0.2

FIG. 10

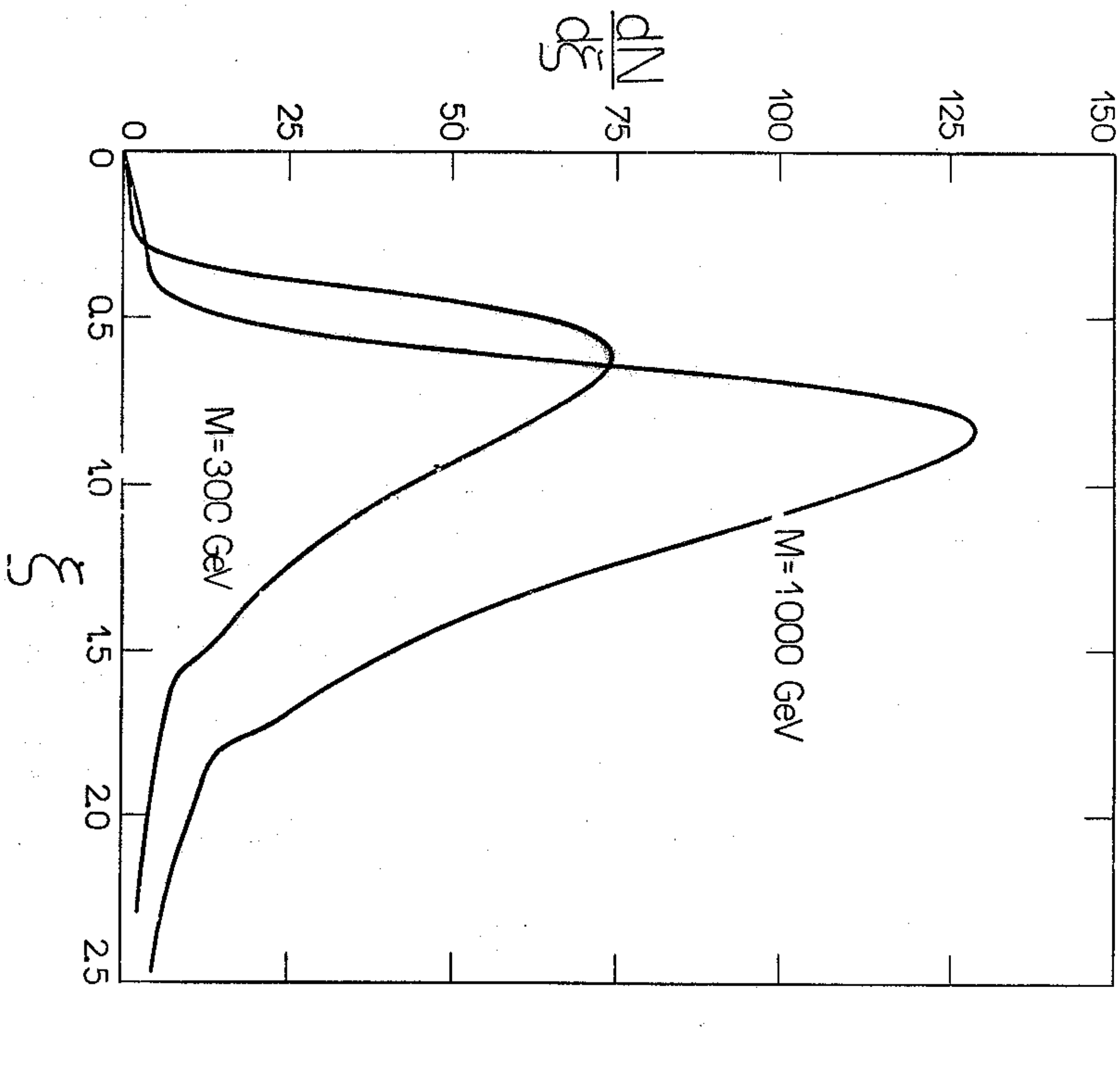

dN/dξ
0
25
50
75
100
125
150
ξ
0
0.5
1.0
1.5
2.0
2.5
M=300 GeV
M=1000 GeV

FIG. 11